AN APFIM STUDY OF THE AGEING BEHAVIOUR OF U-6.0 wt% Nb

G. Beverini, D. Edmonds

COLLOQUE DE PHYSIQUE
Colloque C8, Supplément au n°11, Tome 50, novembre 1989

AN APFIM STUDY OF THE AGEING BEHAVIOUR OF U-6.0 wt% Nb

G. BEVERINI and D.V. EDMONDS

Department of Metallurgy and Science of Materials, University of Oxford, Parks Road, GB-Oxford OX1 3PH, Great-Britain

Abstract. Atom Probe Field Ion Microscopy (APFIM) in conjunction with Transmission Electron Microscopy is being used to determine the mechanisms responsible for the strength increase observed upon ageing U-6.0wt% Nb. Analysis of composition profiles obtained from the APFIM show that two distinct types of phase separation reactions are taking place during ageing. At present no conclusive evidence exists to identify the reaction mechanisms. However, electron diffraction and APFIM results suggest that at ageing temperatures below 400°C a fine scale segregation reaction takes place, possibly spinodal decomposition, whilst at temperatures above 400°C strengthening is probably due to precipitation of a Nb-rich phase.

1 - INTRODUCTION

Depleted uranium alloys are very attractive for non-nuclear engineering applications that can exploit their high density, availability, and low cost (1). U-6Nb alloy, the most ductile of all the heat treatable uranium alloys is usually used in applications in which a balance of high ductility and moderate strength is needed. To achieve this balance of mechanical properties U-6Nb is water quenched (WQ) from the solutionising temperature and aged at relatively low temperatures (2). On quenching from the solutionising temperature a supersaturated martensite variant of α uranium is formed designated α_b". α_b" is a soft and ductile heavily twinned banded martensite possessing a monoclinic crystal structure (3). Ageing this microstructure can result in large strength increases and severe ductility losses. At present no definitive explanation exists for the strengthening developed during ageing. Jackson (4) suggests that strengthening at temperatures above 400°C results from precipitation of α (pure U) on twin boundaries or dislocations and strengthening below 400°C results from a segregation reaction possibly spinodal decomposition. X-ray diffraction and TEM work performed by Eckelmeyer and coworkers (5) supports Jackson's hypothesis that strengthening at ageing temperatures below 400°C is due to a fine scale segregation reaction consistent with spinodal decomposition. Kinetics of strengthening work performed by Eckelmeyer (6) on aged U-4.0wt% Nb alloy having the same α_b" microstructure in the as WQ condition suggests that strengthening is due to segregation of impurity atoms to twin interfaces. Overaging in U-6Nb is due to the discontinuous or cellular precipitation of the equilibrium microstructure at prior γ grain boundaries. The equilibrium microstructure consists of a lamellar two phase mixture of α plus γ_2 (approx. 55wt%Nb) (4).

Lack of substantial evidence supporting the strengthening mechanisms suggested is mainly due to the fine scale of the reaction and to uranium's low electron transparency and high oxidation rate. APFIM is one of the few techniques which can provide high resolution morphological and micro-analytical details needed to determine the mechanism responsible for the strength increase observed. APFIM has been successfully used to study the ageing behaviour of uranium - 0.75wt% titanium and uranium - 2.2wt% molybdenum alloys (7). This investigation uses Oxford University's VG FIM 100 Atom Probe and JEOL JEM 4000EX Transmission Electron Microscope to examine the microstructural and chemical changes occurring upon ageing U-6Nb alloy.

2 - EXPERIMENTAL

APFIM. Specimens were prepared from machined 1mm diameter 12mm long WQ and aged rods via a two stage electropolishing technique. In the first stage the diameter of the rods was reduced to approximately 0.3mm and necked. This was achieved by electropolishing the rods in an electrolyte (25% HClO - 75% $HC_2H_3O_2$) floating on an inert denser liquid. In the second stage the tip was formed by electropolishing the necked blank in a circulating solution of 6% perchloric acid, 34% n-butyl alcohol and 60% methanol cooled to -27°C. An electropolishing cell identical to that used by Hadjadj et al (8) to manufacture titanium FIM specimens was used to carry out the second stage of the specimen preparation process.

Even though specimens were placed in the ultra high vacuum of the FIM immediately after preparation, they were found to be heavily oxidized. The oxide was removed in the FIM by field evaporation in the presence of argon image gas at a temperature of 80K. Once the oxide layer was removed imaging of the metal surface was carried out using neon as imaging gas at temperatures between 50K and 70K. AP analysis was performed with or without imaging gas at 70K at a pulse fraction of 15%. All statistical analysis of APFIM results were performed using a sample and step size of 100 ions unless otherwise stated.

AP analyses performed on WQ, and WQ and aged U-6Nb alloy revealed that the material used contained no significant amounts of carbon or oxygen interstitial impurities (less than 0.1at%). Hydrogen was found in the AP analyses performed however, it is impossible to conclude if there is segregation of this element at twin interfaces.

3 - RESULTS

No phase contrast was observed in the FIM images of aged material therefore this discussion is based solely on TEM results and statistical analysis of data from AP results.

Figure 1 shows the effect of ageing time at various temperatures on Vickers hardness. Sample distribution analysis performed on random area AP results of WQ U-6Nb revealed a non-random distribution of Nb in the specimen (Fig. 2a). Black bars represent the actual distribution and white bars represent a binomial distribution of the same mean composition. This non-randomness does not take the form of periodic composition fluctuations as seen by the autocorrelation analysis shown in figure 2b. Figure 2c shows the heavily twinned banded α_b" martensite obtained upon quenching U-6Nb alloy. No evidence of phase separation was found on TEM work performed on the quenched alloy.

Figure 3a is a bright field TEM micrograph of material aged 1 hr. at 400°C showing the aged α_b" matrix. The structure no longer contains the fine array of transformation twins within the martensite bands shown in figure 2c. Instead of the transformation twins the bands contain a fine dispersion of unidentified plates or rods. Figure 3b is a dark field TEM micrograph illuminating the particles in figure 3a. Figure 4 is a BF TEM micrograph of the lamellar decomposition product found at prior γ grain boundaries in material aged for 1 hour at 400°C. Figure 5 is an optical micrograph of material aged for 1 hr. at 400°C showing prior γ grain boundaries coated with the equilibrium decomposition product. Figure 6 shows a BF TEM micrograph of material aged for 16 hrs. at 300°C. The microstructure consists of martensite bands containing wavy irregular plates or rods of approximately 4nm in thickness. Similar microstructures have been observed by Livak and Thomas (9), and Butler and Thomas (10) in spinodally decomposed Cu-Ni-Fe alloys. No lamellar decomposition product was found in material having this heat treatment. TEM work has not yet been performed on material aged at 450°C.

Due to the fine scale of the phase separation reaction, and the difficulty of performing electron diffraction experiments of decomposed alloys containing phases of similar crystal structures, characterization of the decomposition reaction is carried out using the atom probe.

Figure 7 shows a section of a composition profile obtained from random area AP analysis performed on material aged at 400°C for 1 hour. Figure 8 shows the frequency distribution of the profile shown in figure 7, a non-random Nb distribution is observed. There appears to be composition fluctuations of two different dimensions as shown in figure 7, one is of the order of 3 to 4 nm. and the other is of the order of 10 to 15 nm. Autocorrelation analysis, shown in figure 9, revealed the larger fluctuations since the first minimum occurs at 12 nm. This is always the case for alloys having a range of particle sizes since this analysis is biased towards larger particles.

Figure 10 shows a section of the composition profile obtained from random area AP analysis performed on material aged 16 hours at 300°C. This composition profile only shows one composition fluctuation size, as opposed to that of figure 7, of the order of 3 nm. The frequency distribution of this composition profile also revealed a non-random Nb distribution (figure 11). Autocorrelation analysis performed on the composition profile revealed the fine composition fluctuations (figure 12). The particle size calculated from this figure yielded a value of approximately 3 nm. The same argument applies for this case as for the previous autocorrelation analysis.

Figure 13 shows a portion of the composition profile from material aged at 450°C for 30 mins. Sample distribution analysis performed on this composition profile also revealed a non-random Nb distribution (figure 14). This concentration profile shows widely separated high Nb concentration spikes

4 - DISCUSSION

It is clearly seen from figure 3 that orientation of the FIM tips is important to determine the exact dimensions of the particles in the volume analysed. Unfortunately no crystallographic information can be obtained from the FIM images and due to uranium's low electron transparency observation of tips prior to probing using a TEM is impossible.

The particle dimensions obtained from AP analysis performed on material aged for 1 hr. at 400°C could correspond to both the decomposed α_b" matrix shown in figure 3 (if particles are transversed at angles lower than 45°) or the lamellar decomposition product shown in figure 4. Probability of the lamellar decomposition product forming part of the APFIM tips is low due to its low volume fraction (figure 5) although, it should be noted that preferential polishing of the lamellar microconstituent has been observed when preparing TEM samples.

The material aged for 16 hrs. at 300°C does not contain the lamellar microconstituent. APFIM results correlated well with TEM results since in both cases the particle size obtained was approximately equal to 3 nm. Both TEM and APFIM results suggest that decomposition at 300°C is consistent with spinodal decomposition and the elongation of particles observed indicates that elastic anisotropy is important in determining their morpholgy. More statistical analysis of APFIM results is required to confirm this theory.

Comparison of APFIM results of material aged 30 mins. at 450°C with those of material aged at lower temperatures suggests that different kinetics of phase separation occur at the higher temperatures. The widely spaced high Nb concentration spikes suggest that strengthening at this temperature is due to classical nucleation and growth of precipitates.

5 - SUMMARY

The APFIM and TEM results suggest that a single mechanism, phase separation is responsible for strengthening. However there may be two different regimes at low and high ageing temperatures. At temperatures above 400°C strengthening could take place through precipitation of Nb-rich particles. At temperatures below 400°C

phase separation consistent with spinodal decomposition could be taking place. No evidence was obtained to suggest that strengthening occurs via segregation of impurity interstitial atoms to twin interfaces. Further work is in progress to clarify these issues.

6 - ACKNOWLEDGEMENTS

This research is supported by the Procurement Executive, Ministry of Defence. Acknowledgement is made to Professor Sir Peter Hirsch FRS for provision of laboratory facilities . Dr G.D.W. Smith is thanked for the use of the APFIM equipment and Dr. A. Cerezo and Dr. M.G. Hetherington for help with APFIM techniques. Miss B.A. Shollock is also thanked for use of the electropolishing unit. Finally Mr. T.J. Godfrey is gratefully acknowledged for constant help during use of the APFIM equipment.

7 - REFERENCES

[1] Tardiff, H.P., Can. Min. Bull. **58** (1965) 1167.
[2] Jackson, R.J. and Miley, D.V., Trans. ASM **61** (1968) 337.
[3] Eckelmeyer, K.H., Metals Handbook, **9** (1985) 476.
[4] Jackson, R.J., Dow Chemical Company, Rocky Flats Division, Golden, Colo., U.S Atomic Energy Commission Contract Report No. AT(29-1)-1106 (1971).
[5] Eckelmeyer, K.H., Romig, A.D., and Weirick, L.J., Met Trans, **15A** (1984) 1319.
[6] Eckelmeyer, K.H., in 'Physical Metallurgy of U Alloys', Burke, J.J. et al., eds.,Chestnut Hill, Mass. (Brook Hill) 1976, 463.
[7] Jenkins, B.A. and Edmonds, D.V., J. de Physique **48** (1987) C6-277.
[8] Hadjadj, L., Menand, A. and Blavette, D., J. de Physique **47** (1986) C7-281.
[9] Livak, R.J. and Thomas G., Acta Met. **19** (1971) 497.
[10] Butler, E.P. and Thomas G., Acta Met. **18** (1970) 347.

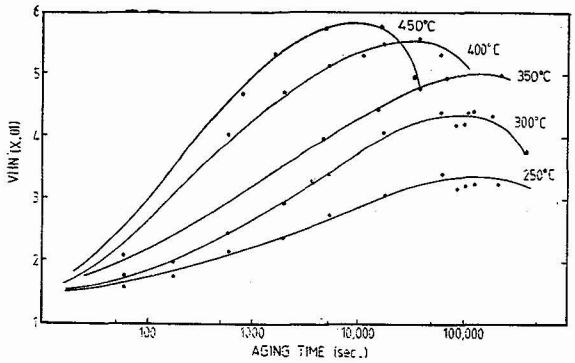

Fig. 1: Ageing behaviour of U-6Nb at various temperatures.

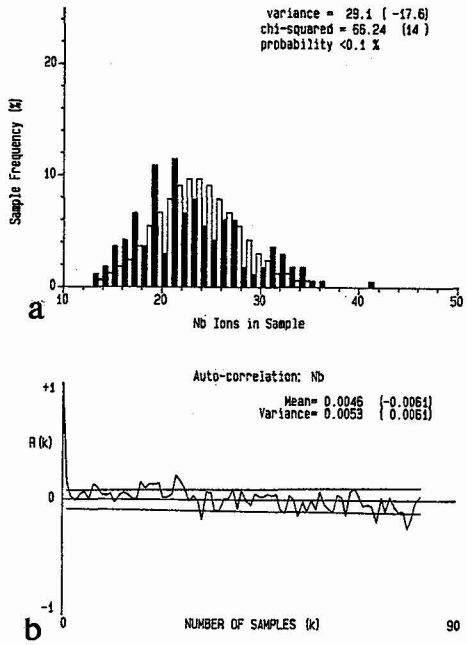

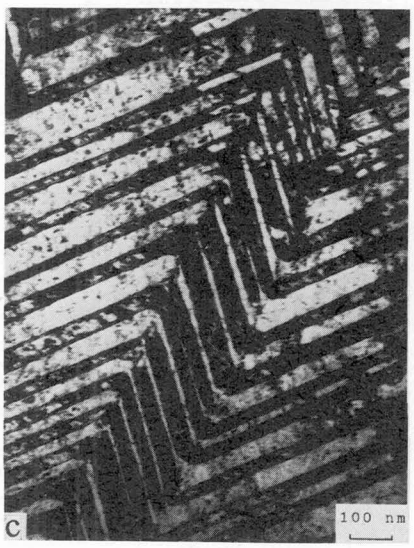

Fig. 2: (a) Frequency distribution, (b) autocorrelation analysis, and (c) BF TEM micrograph showing α_b" microstructure: WQ U-6Nb alloy.

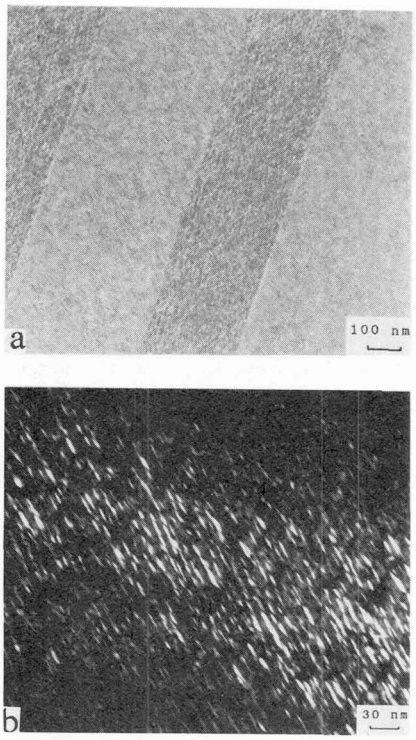

Fig. 3: (a) BF TEM micrograph of U-6Nb aged hr. at 400°C showing fine dispersion of particles within martensite plates, (b) D TEM micrograph illuminating particles.

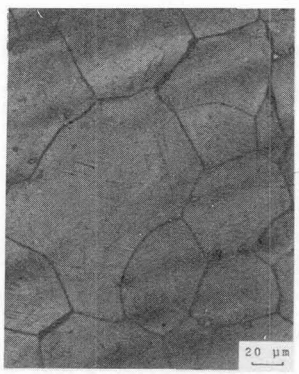

Fig. 5: Optical micrograph of U-6Nb aged 1 hr. at 400°C, showing prior γ grain boundaries coated with decomposition product.

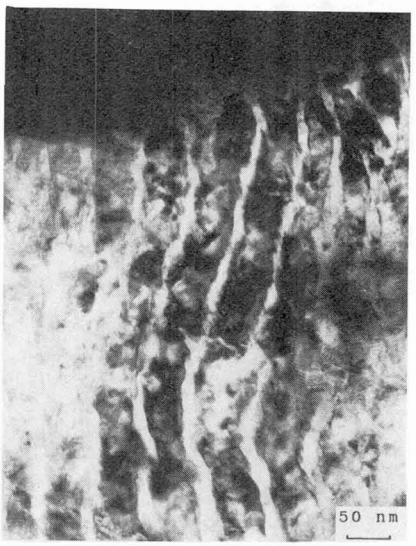

Fig. 4: BF TEM micrograph showing lamellar decomposition product in material aged 1 hr. at 400°C.

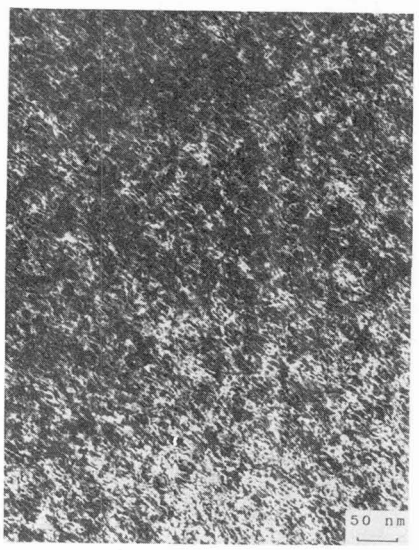

Fig. 6: BF TEM micrograph showing fine modulated structure in material aged 16 hrs. at 300°C.

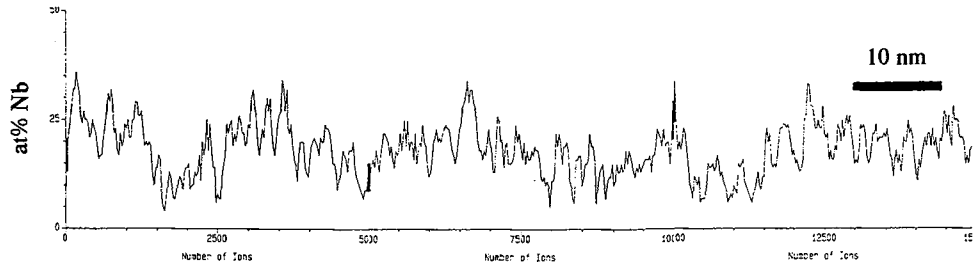

Fig. 7: Concentration profile of material aged 1 hour at 400°C (Sample size: 100, Step Size: 25).

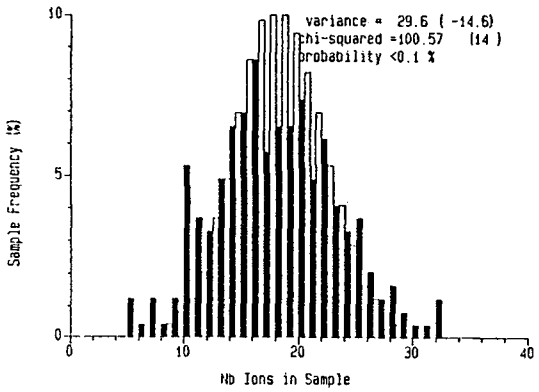

Fig. 8: Frequency distribution of material aged 1 hour at 400°C.

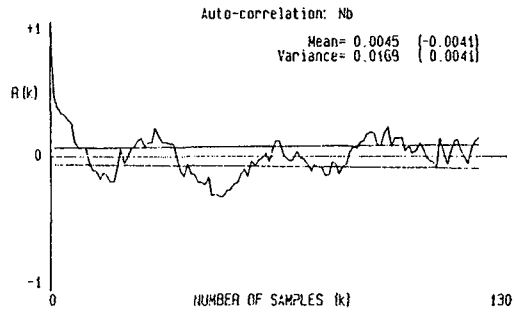

Fig. 9: Autocorrelation analysis of U-6Nb aged 1 hr. at 400°C.

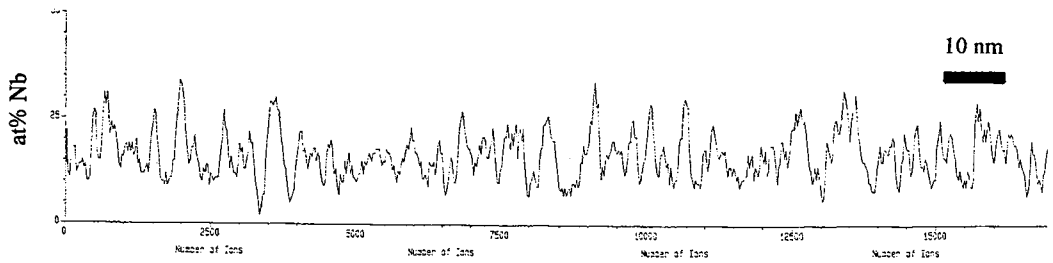

Fig. 10: Concentration profile of material aged 16 hrs. at 300°C (Sample size: 100, Step Size: 25).

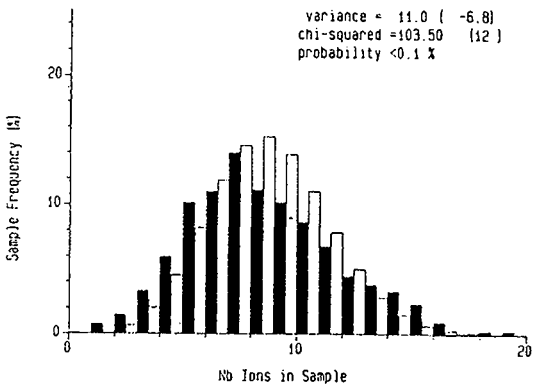

Fig. 11: Frequency distribution of material aged 16 hrs. at 300°C (Sample size: 50, Step size: 50).

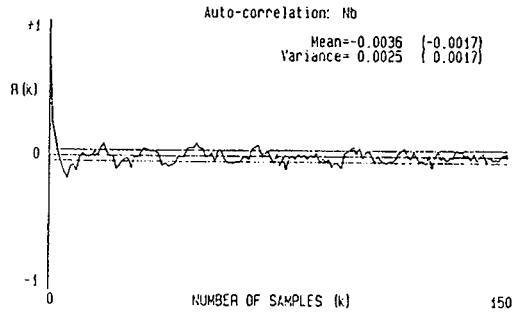

Fig. 12: Autocorrelation analysis of material aged 16 hrs. at 300°C (Sample size: 50, Step size: 50).

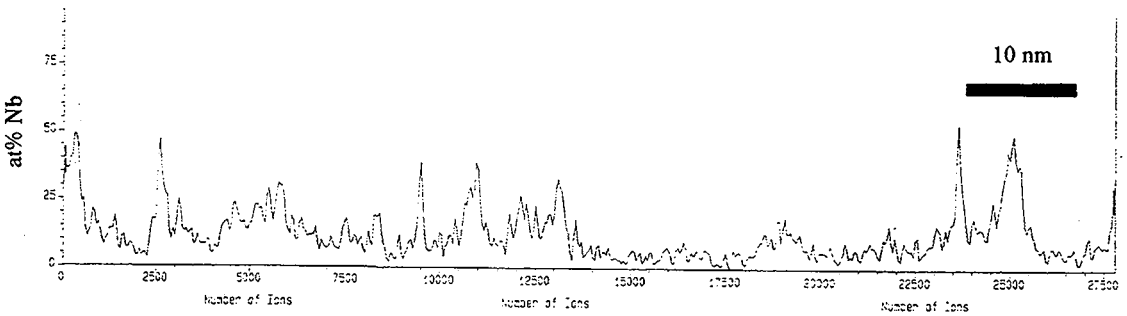

Fig. 13: Concentration profile of material aged 30 mins at 450°C (Sample Size: 100, Step Size: 25).

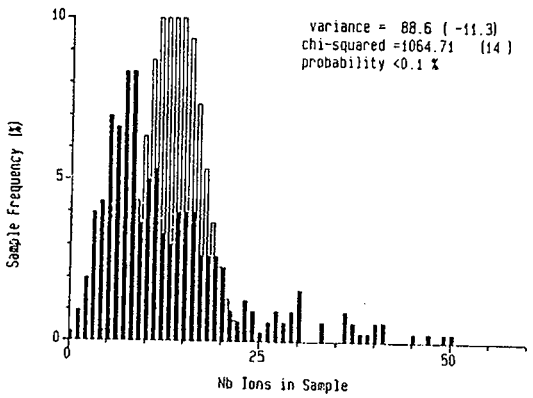

Fig. 14: Frequency distribution of material aged 30 mins. at 450°C.